Thermal Performance of Rubberized Gypsum Composites for Sustainable Walls in Arid Climates: Experimental and Simulation Study

Hamza Laoubi[1]; Abdelaziz Meddah[2]; Madani Bederina[3]; and Abd Elmalik Goufi[4]

Abstract: This study evaluates the potential of rubberized gypsum composites as sustainable wall materials for improving energy efficiency in buildings located in arid climates, using M'sila, Algeria, as a representative case. The novelty of the work lies in the dual experimental and simulation-based analysis of recycled rubber waste (RW) incorporation, specifically addressing thermal comfort under arid climatic conditions. Natural sand was partially replaced with recycled RW at levels of 0%–50% by volume. Laboratory experiments quantified the effects of RW on the mechanical strength, density, and thermal properties, while simulations assessed the thermal insulation of walls under arid conditions. Key parameters included wall configuration (single/double layer), thickness, air cavity integration, and surface coatings. The results showed that increasing RW content reduced mechanical strength and density but significantly improved, the thermal insulation performance of the composite with thermal conductivity decreasing by 52% at 50% RW. Simulations revealed that thicker walls with integrated air cavities and coated surfaces enhanced thermal inertia, increasing time lag (φ) and reducing decrement factor (f). These design strategies stabilize indoor temperatures and mitigate peak heat fluxes, thereby reducing energy demand. By valorizing nonbiodegradable waste, the proposed composites lower costs, reduce embodied energy, address RW disposal challenges, and offer practical solutions for climate-responsive, sustainable buildings in arid regions. **DOI: 10.1061/JAEIED.AEENG-2144**. © *2026 American Society of Civil Engineers*.

Practical Applications: This study introduces gypsum composites modified with recycled rubber waste (RW) as an eco-friendly wall material for buildings in arid regions. By partially replacing natural sand with RW, the composite improves thermal insulation while reducing reliance on nonrenewable resources. Although the addition of rubber decreases mechanical strength, it significantly enhances energy performance by lowering thermal conductivity and stabilizing indoor temperatures. For practitioners, this means walls built with rubberized gypsum can reduce cooling energy demand during hot seasons by delaying and reducing heat transfer through building envelopes. The study also shows that practical design choices, such as wall thickness, adding air cavities, and surface coatings, further improve thermal inertia, making these materials suitable for low-cost housing and sustainable construction projects. Beyond performance, this approach provides a viable recycling solution for rubber waste, helping address disposal challenges while lowering costs and embodied energy. Engineers, architects, and builders can adopt these composites to create climate-responsive buildings that enhance occupant comfort, reduce operational energy use, and contribute to environmental sustainability in regions facing extreme heat.

Author keywords: Gypsum composites; Rubber waste recycling; Thermal inertia; Sustainable construction; Energy efficiency; Arid climate construction.

Introduction

According to the United Nations Environment Programme (UNEP 2025), the building sector is responsible for 34% of global energy-related CO_2 emissions and 32% of global final energy consumption. Furthermore, its significant reliance on materials such as cement and steel accounts results in approximately 18% of global CO_2 emissions from production processes and contributes substantially to construction waste. To address this, the European Union has prioritized improving the thermal performance of building envelopes as a cost-effective strategy to reduce energy demands in extreme climates. This initiative aligns with global efforts to replace conventional construction materials with sustainable alternatives that minimize environmental impact, conserve natural resources, and enhance energy efficiency (Berardi et al. 2018; Merniz et al. 2025). In this sense, the 2015 Paris Climate Accord set the goal of limiting global warming to below 2°C, ideally 1.5°C. Reaching this target requires a shift to a low-carbon economy through renewable energy investment, clean technologies, sustainable lifestyles, and improved energy efficiency, particularly in high-emission sectors (Soussi et al. 2024).

In Algeria, rapid urbanization has intensified energy consumption in the building sector. To mitigate this, national strategies aim to reduce CO_2 emissions by 193 million t by 2030, partly through the adoption of insulating materials that lower heating

[1]Dept. of Civil Engineering, Univ. of Mohamed El Bachir El Ibrahimi of Bordj Bou Arreridj El-Anasser, Bordj Bou Arreridj 34030, Algeria. ORCID: https://orcid.org/0000-0002-9262-6726. Email: hamza.laoubi@univ-bba.dz

[2]LDGM, Dept. of Civil Engineering, Univ. of M'sila, Bordj Bou Arreridj Rd., 28000 M'sila, Algeria (corresponding author). ORCID: https://orcid.org/0000-0002-6855-5331. Email: abdelaziz.meddah@univ-msila.dz

[3]Dept. of Civil Engineering, Univ. of Lagouhat, Université Amar Telidji, 37G Route de Ghardaia–Laghouat, Laghouat 03000, Algeria. Email: m.bederina@lagh-univ.dz

[4]Dept. of Civil Engineering, Univ. of Mohamed El Bachir El Ibrahimi of Bordj Bou Arreridj El-Anasser, Bordj Bou Arreridj 34030, Algeria. Email: abdelmalik.goufi@univ-bba.dz

Note. This manuscript was submitted on June 12, 2025; approved on November 7, 2025; published online on January 7, 2026. Discussion period open until June 7, 2026; separate discussions must be submitted for individual papers. This paper is part of the ***Journal of Architectural Engineering***, © ASCE, ISSN 1076-0431.

and cooling demands. The buildings sector currently accounts for approximately 40% of the country's total energy consumption, with heating and cooling representing the major component. The integration of energy-efficient materials, such as insulation, has the potential to reduce heating and cooling demands by 20%–30% and decrease residential energy costs by 15%–20%, thereby contributing significantly to the national CO_2 reduction targets (Ministry of Energy 2015). Lightweight materials with low thermal conductivity, high porosity, and moderate mechanical strength are particularly promising for wall partitions and coatings in energy-efficient designs.

The thermal performance of building envelopes depends critically on material properties and design. As emphasized in the Tackling Climate Change report, optimizing thermal insulation offers the best cost–benefit ratio for energy savings (Al-Jabri et al. 2005; Egenhofer et al. 2006; Guillén et al. 2014; Mavromatidis et al. 2012). Gypsum, a low-cost and widely available material, has gained attention as a sustainable binder because of its inherent thermal and acoustic insulation properties, lightweight nature, and reduced carbon footprint compared with cement (Badens 1998; Ben Mansour et al. 2013). Recent studies have further enhanced the insulation capacity of gypsum by incorporating additives such as plant fibers (Djoudi et al. 2014), expanded polystyrene (Laoubi et al. 2017, 2018), rubber waste (Herrero et al. 2013), and other natural wastes, such as sheep wool, sawdust, and cork granules (Soussi et al. 2024). While these additives reduce mechanical strength, they significantly improve thermal performance, a trade-off that aligns with the requirements of nonstructural insulating materials. Although previous works on gypsum-based systems have mainly focused only on normal weather conditions and emphasized either experimental approach, the present study is based on both experimental investigations and numerical simulations, providing a more comprehensive analysis. This approach allows not only laboratory validation of mechanical and thermal properties but also practical assessment of wall performance under arid climatic conditions, thereby strengthening the novelty and applicability of the findings.

Beyond gypsum-based systems, several other eco-efficient wall solutions have been investigated for sustainable construction such as hempcrete and aerated concrete. Hempcrete, a biobased composite produced from hemp hurds, lime, and water, exhibits excellent insulation capacity ($\lambda \approx 0.09$–0.15 W/m·K) and carbon sequestration potential due to both the natural CO_2 uptake of hemp fibers and the carbonation of lime binders (Steyn et al. 2025). However, its very low compressive strength (0.3–2 MPa), long curing time, and sensitivity to moisture limit its use in non-load-bearing walls. Aerated concrete, by contrast, provides moderate compressive strength (3–7 MPa) and good thermal insulation ($\lambda \approx 0.15$–0.25 W/m·K) but requires energy-intensive production involving autoclaving and foaming processes (Jellen and Memari 2025; Narayanan and Ramamurthy 2000).

In contrast, gypsum–rubber composites offer a regionally adapted and low-energy alternative, relying on locally available gypsum and recycled RW to produce lightweight materials with recycled thermal conductivity and enhanced thermal inertia, which are essential for maintaining indoor thermal stability in arid climates. This balance between local resource utilization, environmental benefit, and climatic performance underscores the practical potential of gypsum–rubber systems as sustainable wall materials for energy-efficient buildings in hot regions.

RW, a nonbiodegradable by-product of industrial processes, is particularly compelling as an additive. Its disposal poses environmental risks, including soil pollution and pest proliferation; however, its resilience, ductility, and waterproofing qualities make it valuable for construction applications. For instance, rubber has been repurposed in concrete (Meddah 2015; Meddah et al. 2014, 2017), gypsum composites (Ferrández et al. 2024), and soil reinforcements (Meddah and Merzoug 2017). Recycling rubber waste in building materials not only addresses waste management challenges but also supports circular economy principles while offering cost benefits by reducing the demand for natural aggregates. This makes RW-based gypsum composites economically attractive, since raw rubber waste has low or even negative acquisition costs due to disposal fees, and its inclusion can simplify constructability through lighter, more workable mixtures.

The M'sila region of Algeria is classified as an arid zone, characterized by extreme diurnal temperature fluctuations: scorching daytime heat (exceeding 40°C in summer) and cold nights (dropping below 5°C in winter) (Deghfel et al. 2019). These conditions require building materials with high thermal inertia to delay and dampen heat transfer, thereby stabilizing indoor temperatures and reducing reliance on mechanical cooling/heating. The novelty of the present work lies in combining experimental testing with dynamic simulations to assess how RW and local dune sand can enhance thermal comfort and energy efficiency specifically under arid climatic conditions. For instance, prior studies rarely addressed how RW affect φ (the delay for heat to traverse a wall) or f (the reduction in heat wave amplitude), which are critical metrics for energy efficiency in arid regions like M'sila. Furthermore, the region's abundant dune sand, a fine-grained and underutilized local resource, offers untapped potential to reduce material costs and carbon footprint when combined with RW. This study bridges these gaps by (1) developing a sustainable gypsum composite using recycled rubber waste (0%–50%) and dune sand; (2) quantifying trade-offs between rubber content, mechanical strength, and thermal properties; (3) evaluating thermal inertia (f, φ) through numerical simulations; and (4) proposing wall configurations (thickness, air cavities, and coatings) to optimize energy efficiency in arid zones.

Materials and Methods

Materials

The gypsum used in this study was provided by a local factory in Ghardaia, Algeria. It is mainly composed of calcium sulfate dihydrate ($CaSO_4 \cdot 2H_2O$), as confirmed by X-ray diffraction analysis (Fig. 1). Chemical analysis revealed that gypsum is predominantly composed of sulfur trioxide (SO_3) and calcium oxide (CaO), consisting of its dihydrate structure, as shown in Table 1. According to the CNERIB (1993) classification, the material falls under Class I gypsum. Particle size distribution analysis, conducted in accordance with NFB 12-301 (AFNOR 1987) standards, showed that 6.9% of the grains exceed 0.8 mm, confirming its classification as coarse gypsum.

Locally sourced dune sand (0/0.63 mm granular class) with a specific density of 2,596 kg/m^3 was used as the primary aggregate. The sand was clean, with negligible organic impurities and low clay content, as indicated in Table 2, making it suitable for composite preparation. X-ray diffraction (XRD) analysis (Fig. 1) confirmed that the sand was predominantly composed of silica (SiO_2), which is characteristic of dune sands from arid regions. Granulometric analysis (Fig. 2) showed that the sand fraction ranged from 0.08 to 0.63 mm, with a median particle size (D_{50}, diameter corresponding to 50% cumulative passing) of approximately 0.35 mm.

Shredded RW particles, supplied by SAEL Factory (Algiers, Algeria), were incorporated as a partial replacement for sand.

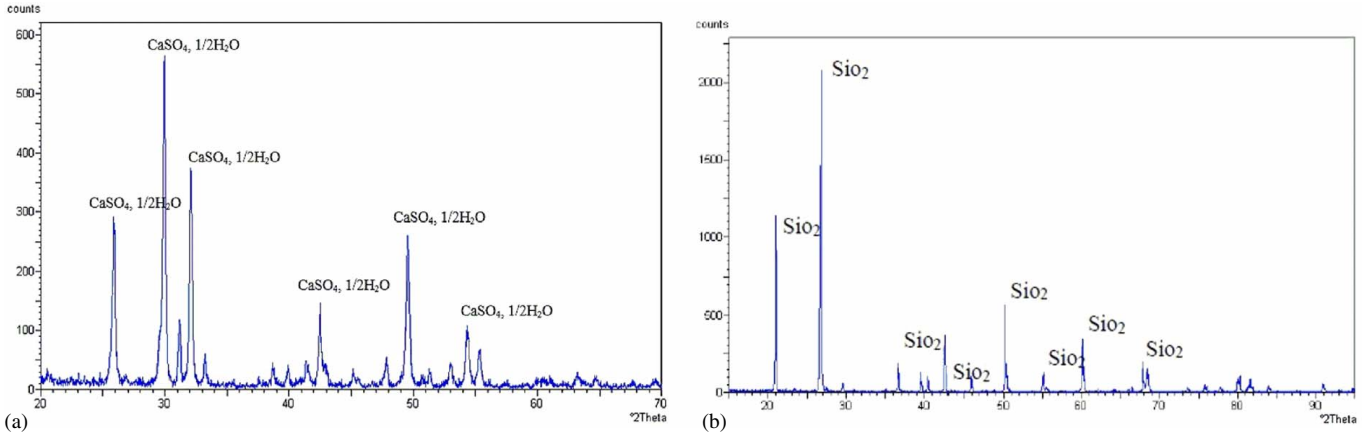

Fig. 1. X-ray diffractogram of (a) plaster; and (b) sand.

RW has a specific density of 1,114 kg/m^3 and irregular morphology, as shown in Fig. 2. Particle size distribution analysis (Fig. 2) indicated a maximum particle size of 8 mm, with a median particle size (D_{50}) of about 6 mm. Compared with the finer dune sand, RW particles are coarser and more irregular in shape, suggesting that they primarily contribute to the granular skeleton of the composite rather than filling fine voids. The irregular shape and low density of rubber can entrap air within the matrix, enhancing thermal insulation, which supports the study's main objective of improving plaster composites' thermal performance.

To extend the setting time and enhance moisture resistance, hydrated lime [$Ca(OH)_2$] was incorporated at 6% by binder mass. This dosage lies within the 4%–8% range recommended by Debouci et al. (1989) for gypsum-based elements used in exterior walls, ensuring both workability and strength. Previous studies have shown that lime additions within this range can refine pore structure, reduce capillary absorption, and increase compressive strength by up to 25% (Salih and Hussein 2018; Walker et al. 2014).

Methods

Thermal Efficiency Analysis

The thermal efficiency of walls is typically evaluated using full-scale experiments or numerical simulations (Neya et al. 2021; Oktay et al. 2016; Quagraine et al. 2020). While in situ testing provides high accuracy, it is costly and time-intensive; thus, this study employed EnergyPlus software (v9.4) for simulation and validated against climatic data from M'sila, Algeria. Key factors that may influence thermal performance, as identified in previous studies (Asan 2006; Belhadj et al. 2020; Fathipour and Hadidi 2017), including the thermophysical properties of materials (conductivity and heat capacity), solar absorptivity and heat storage capacity of wall surfaces, wall orientation, and meteorological data (ambient temperature and solar radiation), were retained in this study.

Thermal inertia is quantified using decrement factor (f) and time lag (φ) as follows:

$$f = \frac{T_{\max}^{(i)} - T_{\min}^{(i)}}{T_{\max}^{(o)} - T_{\min}^{(o)}} \quad (1)$$

$$\varphi = t_{T_{\max}^{(i)}} - t_{T_{\max}^{(o)}} \quad (2)$$

where $T_{\max}^{(o)}$ and $T_{\min}^{(o)}$ = maximum and minimum temperatures on the outer wall surface, respectively; and $T_{\max}^{(i)}$ and $T_{\min}^{(i)}$ = maximum and minimum temperatures on the inner wall surface, respectively.

A unidirectional heat transfer model was assumed, consistent with standard wall analysis practices (Oktay et al. 2016). Simulations used a $3 \times 2 \times 2$ m^3 test room (Fig. 3), inspired by prior studies (Erell and Etzion 1992; Zhang et al. 2006), with walls modeled as multilayered systems including air gaps (DTR C3-2, CNERIB 1997) $t_{T_{\max}^{(i)}}$ and $t_{T_{\max}^{(o)}}$ Time (hours) to reach peak temperatures on inner/outer surfaces.

Table 1. Chemical composition of plaster used

Element	Percent
SiO_2	0.7
Al_2O_3	0.1
Fe_2O_3	0.08
CaO	36.15
MgO	0.53
SO_3	52.95
Cl	0.02
KO	0.03
Na_2O	0.09
LOI	5.59

Material Preparation

The composite mixes were designed according to Algerian CNERIB specifications (CNERIB 1993):

- Water/gypsum ratio (W/P): 0.6.
- Gypsum/sand ratio (P/S): 0.5 (higher ratios degrade mechanical properties (Djoudi 2015).

Recycled RW was incorporated by partial replacement of the volume of sand at 10%–50%. The mixing procedure was inspired by a previous study (Laoubi et al. 2019).

- Dry components (gypsum, sand, and RW) were blended for 30 s.
- Water was gradually added, with continued mixing for 30 s.

Prismatic samples ($40 \times 40 \times 160$ mm^3) and cubes ($40 \times 40 \times 40$ mm^3) were cast; cured for 7, 14, and 28 days at 20°C ± 1°C

Table 2. Physical properties of sand

Property	Value
Specific density (kg/m^3)	2,596
Apparent density (kg/m^3)	1,428
Porosity (%)	45
Sand equivalent (%)	86
Organic impurities (%)	<0.5
Clay content (%)	<1.5

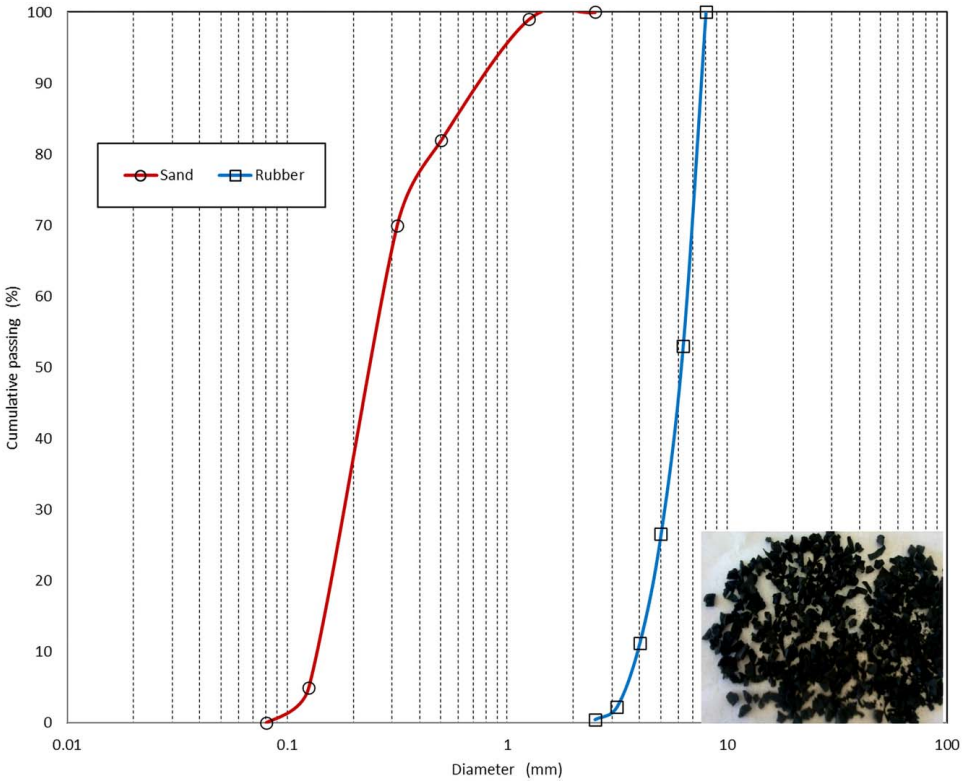

Fig. 2. Particle size distribution and general appearance of recycled RW.

and 45% ± 1% RH; and tested for flexural/compressive strength per NF-EN 13279-2 (CEN 2014).

Thermal and Mechanical Testing

Thermal properties (conductivity, diffusivity, and heat capacity) were measured using the transient plane source (TPS) method (Fig. 4). A TPS probe, sandwiched between two sample halves, recorded temperature-dependent resistance changes in a Wheatstone bridge circuit. Data were analyzed using ISO 22007-2 (ISO 2015) protocols. The mechanical strength was assessed using a universal testing machine. For flexural strength, three-point bending on $40 \times 40 \times 160$ mm^3 prisms was used, whereas for compressive strength, $40 \times 40 \times 40$ mm^3 cubes were used, as per NF-EN 13279-2 (CEN 2014).

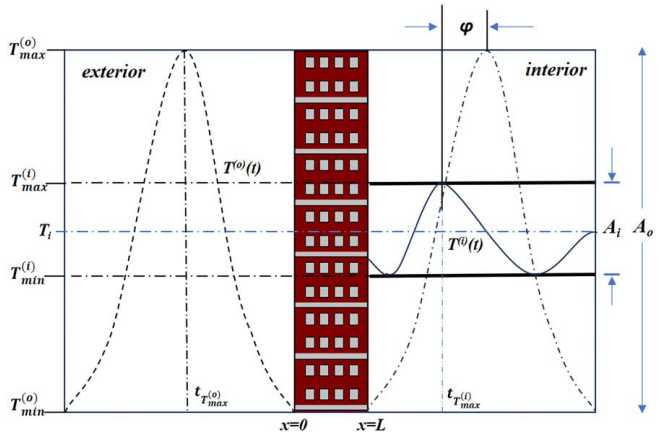

Fig. 3. Schematic representation used for the calculation of time lag and decrement factor.

Results and Discussions

Experimental Characterization

Mechanical Properties

Table 3 summarizes the compressive and flexural strengths of rubberized gypsum mortars, showing that rubber incorporation reduces both compressive and flexural strengths. A clear reduction in both properties is observed as the RW content increases. After 28 days, the compressive strength decreased from 9.95 for the reference mix to 2 MPa at 50% RW, corresponding to nearly 80% loss in strength. This decrease can be is attributed to the low stiffness of rubber compared to mineral aggregates, the reduction in the load-bearing solid fraction due to partial sand replacement, and the formation of stress concentrations at rubber–gypsum interfaces under load. Furthermore, weak interfacial adhesion between the gypsum matrix and rubber grains further promotes particle debonding during cracks. However, despite the reduction in strength, the mortars exhibited improved ductility relative to reference mix. This enhanced deformability, consistent with earlier studies (Eldin and Senouci 1993; Herrero et al. 2013; Ho Anh Cuong 2010; Raghavan et al. 1998; Jiménez Rivero et al. 2014), reflects a higher energy absorption capacity. From an application standpoint, this property could be advantageous in nonstructural elements where crack resistance under cyclic thermal or mechanical stresses is desirable.

Thermal Properties

The effect of RW content on the thermal properties of gypsum composites was evaluated through thermal conductivity, thermal diffusivity, and specific heat capacity. The relationship between RW content and thermal conductivity is illustrated in Fig. 5. Incorporation of RW significantly reduced conductivity, with a 52% decrease (from 0.615 to 0.296 W/m·K) at 50% replacement. This reduction is attributed to the inherently low conductivity of rubber,

Fig. 4. Experimental setup used for the measurement of the thermal properties.

Table 3. Mechanical properties of composites

Rubber content (%)	Density (kg/m^3)	Compressive strength[a] (MPa)			Flexural strength[a] (MPa)		
		7 days	14 days	28 days	7 days	14 days	28 days
0	1,557.34	5.64	7.02	9.95	2.65	3.73	5.7
10	1,575.22	1.8	2.8	5	1.01	1.67	2.63
20	1,467.2	1.43	2.44	4.51	1.3	1.6	2.44
30	1,459.91	1.31	1.66	3.74	0.86	1.28	1.66
40	1,450.43	1.13	1.55	2.69	0.73	1.02	1.55
50	1,340.37	0.98	1.34	2	0.5	0.66	1.34

[a]Values represent the mean of three independent measurements. The variability was within ±2%, which is considered negligible compared to the accuracy of the testing methods.

the increased closed porosity associated with its irregular particles, and the lower bulk density of RW compared to sand (1,114 versus 2,596 kg/m^3 for sand) (Herrero et al. 2013; Jiménez Rivero et al. 2014).

Thermal diffusivity and specific heat capacity results are summarized in Table 4. Increasing RW content reduced diffusivity by up to 88.6% (from 1.544 to 0.176 mm^2/s), demonstrating that heat propagation through the composites slows markedly as rubber is introduced. In contrast, specific heat capacity increased by 155% (from 0.54 to 1.38 J/kg·K), reflecting an enhanced capacity to store heat.

The combined reduction in conductivity and diffusivity, together with the rise in heat capacity, shows that rubberized gypsum composites act as more effective thermal insulators. These improvements point to potential benefits for lightweight interior applications, particularly in arid climates where reducing energy demand for heating and cooling is a priority.

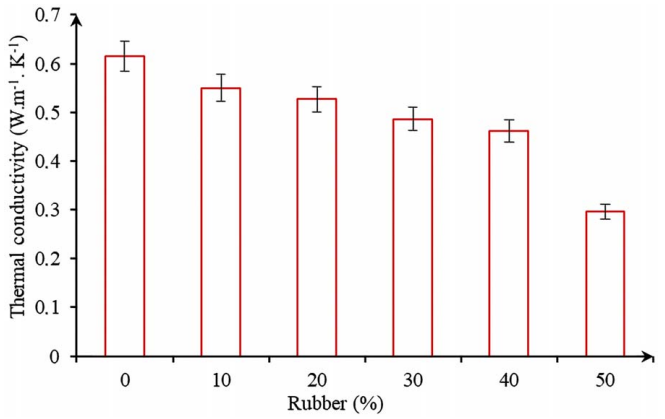

Fig. 5. Variation of thermal conductivity of composites as a function of rubber content.

Simulation

To assess the thermal performance of rubberized gypsum walls in stabilizing indoor temperatures in arid climates, numerical simulations were conducted using experimental thermal property data. A test cell (3 m depth × 2 m width × 2 m height), modeled after validated designs from previous studies (Belhadj et al. 2015; Zhang et al. 2006), was simulated with a south-facing single-glazed window (1 × 0.7 m) to account for solar exposure. Hourly temperatures were tracked at three points: the outer wall surface, inner wall surface, and indoor air.

The external climate inputs (temperature, solar radiation, and wind speed) were taken from the EnergyPlus typical meteorological year weather file for M'sila, Algeria. The indoor air was modeled as a free-floating zone without HVAC systems, infiltration, or internal gains, so that indoor temperature responded naturally to external conditions. This approach isolates the effect of wall thermal properties and geometry from other heat sources. Consequently, the decrement factor (f) and time lag (φ) values reported in this study reflect solely the envelope's dynamic response to the external climate. The boundary conditions and climatic inputs applied in all simulations are summarized in Table 5.

Fig. 6 schematically illustrates the three configurations analyzed in the simulations:

- Fig. 6(a) shows the effect of varying wall thicknesses (10, 15, 20, and 25 cm) for different orientations (north, east, south, and west).
- Fig. 6(b) compares a single 20 cm wall with a double-layer wall including a 5 cm air cavity, keeping total material volume constant.

Table 4. Thermal properties of the different studied mixes

Rubber content (%)	Diffusivity ($m^2 s^{-1}$)	Heat capacity ($J kg^{-1} k^{-1}$)
0	1.544	0.54
10	0.454	0.83
20	0.291	1.03
30	0.301	1.14
40	0.327	1.27
50	0.176	1.38

- Fig. 6(c) represents the same double-layer wall with additional 1 cm gypsum and cement coatings for interior and exterior facets, respectively, highlighting the practical implementations of surface treatments.

Case of Single Wall (Effect of Wall Thickness)

Fig. 7 presents the simulated temperature variations at the outer and inner surfaces for walls of different thicknesses (10–25 cm). the results show that as the thickness increases, the amplitude of inner surface temperature decreases, while the minimum temperature rises. For instance, west-facing walls exhibit a noticeable reduction in outer surface temperature fluctuations, with peak external temperatures reaching 55.5°C, while the internal surface temperatures remain significantly lower: 43.06°C for a 10 cm wall and 35.6°C for a 25 cm wall. The figure also makes evident that orientation strongly affects thermal response. Peak temperatures occurred at distinct times depending on orientation: 14:00 (south), 16:00 (north and west), and 08:00 (east). With increasing wall thickness, peak temperatures are not only reduced but also delayed. This delay is particularly visible in Fig. 7, where west facing walls show progressively later peaks as thickness increases.

As illustrated in Fig. 8, a strong positive correlation between wall thickness and time lag (φ) was obtained. Thicker walls (25 cm) reached φ values of 13 h (east), 10 h (south), 8 h (west), and 7 h (north), while thinner walls (10 cm) only achieved 2–8 h. In terms of decrement factor, Fig. 9 shows that thicker walls yield much lower values (0.076–0.45), indicating superior damping of outdoor temperature fluctuations.

Taken together, Figs. 6 and 7 demonstrate that wall thickness is a dominant factor in enhancing thermal inertia. Thicker walls attenuate external heat loads more effectively and delay heat ingress, while rubber incorporation (as evidenced in Fig. 5) further reduces conductivity. This combined effect validates the use of rubberized gypsum in energy-efficient wall systems for arid climates, particularly for solar-exposed orientations such as the south and west.

Table 5. Boundary conditions and key assumptions adopted for simulations

Parameter	Value or description
Exterior boundary	Outdoor: external environment considering climatic data of M'sila region (temperature, solar radiation, and wind)
Interior boundary	Zone air node (free-floating): indoor temp responds naturally to isolate material thermal behavior
HVAC loads	None
Infiltration	0.0 ACH (no air leakage modeled)
Internal gains	None (no occupancy, lighting, or equipment)
Simulation period	Representative hot day (July 22, 2018)
Mean maximum air temperature (°C)	38.2
Mean minimum air temperature (°C)	23.3
Mean air temperature (°C)	31.2

Note: ACH = air changes per hour.

Case of Double Wall (Air Cavity)

To evaluate the effect of creating an air space in the wall on the thermal performance of a rubberized plaster-based wall, numerical simulations were performed. In this study, it was assumed that the wall was oriented toward south. For consistency, this case focused on south-oriented walls, as they are the most exposed to solar radiation in arid climates. The differences between the outer and inner surfaces for walls with and without an air cavity were compared in daily hours, and the results obtained are plotted in Fig. 10. These findings prove that the introduction of an air gap into the wall considerably decreased the maximum temperature and increased the minimum temperature. To better appreciate the effect of the air cavity on the thermal efficiency of the wall, the values of the decrement factor and time lag were determined and are presented in Table 6. When a single wall of rubberized gypsum is used, the time lag is about of 7 h, whereas the incorporation of 5 cm of air cavity into the wall increased the time lag by +2 h.

Similar conclusions were drawn in previous studies (Mahlia and Iqbal 2010). The authors indicated that the proper selection of insulating materials, optimization of wall thickness, and inclusion of air gaps into walls reduced the energy consumption and air emissions. In addition, the introduction of a cavity reduces material consumption by about 20% while maintaining the same wall thickness, which is an important sustainability benefit.

The air gap between the two layers of the wall constitutes a thermal barrier against heat transmission (by conduction) through the wall layers. It also functions as a temporary heat reservoir: storing

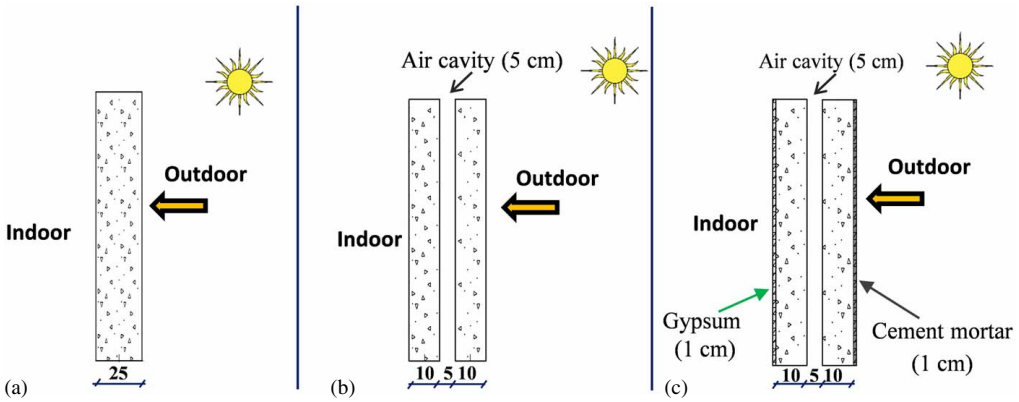

Fig. 6. Configurations of composite walls considered in the study.

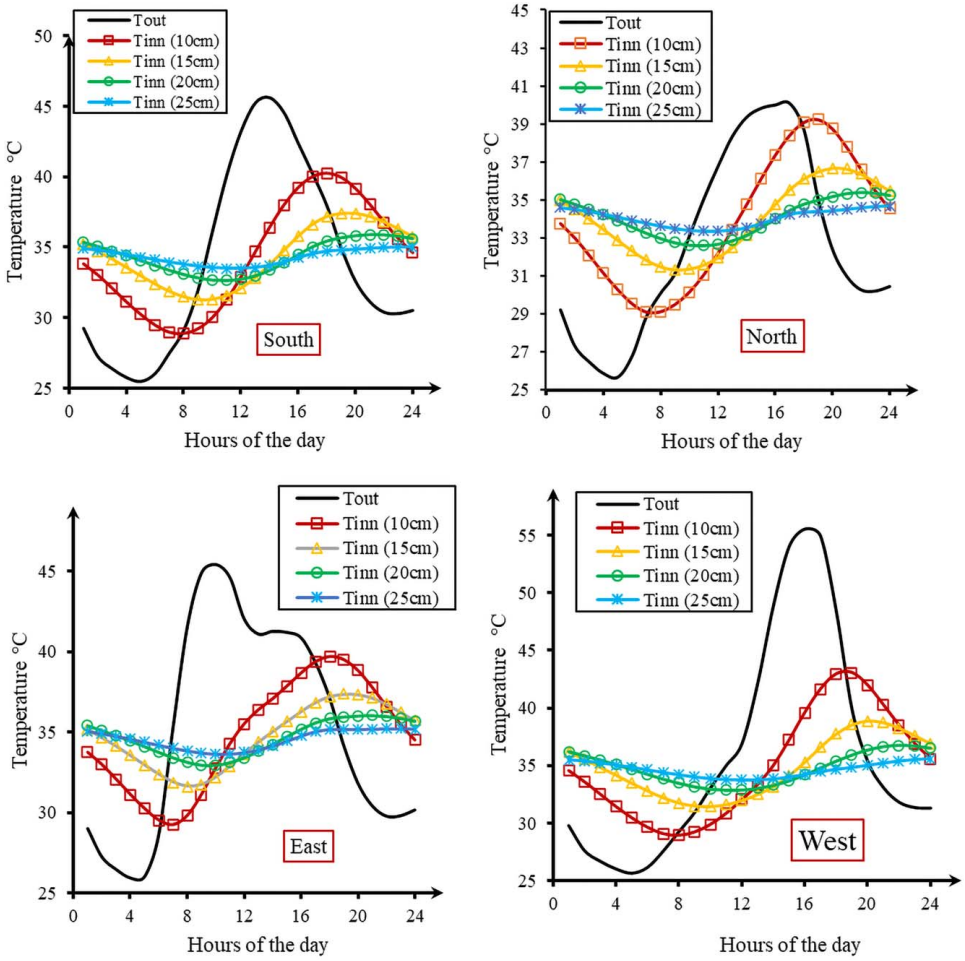

Fig. 7. Effect of wall thickness on daily temperature variations at the exterior and interior wall surfaces.

heat during day and releasing it at night, or vice versa. Therefore, the introduction of an air gap into the wall can reduce energy use in summer and contribute to winter comfort.

Effect of Wall Coating

The effect of using protective surface coating materials for rubberized walls was also investigated. To this end, a thick layer of gypsum mortar (1 cm) was applied on interior side of the rubberized wall, while a cement mortar coating (1 cm) was applied on the exterior side to enhance weather resistance. These coating layers were applied to the double wall stated in the previous section (10 + 5 + 10 cm). The thermophysical properties of coating materials are summarized in Table 7.

The decrement factor (f) and time lag (φ) values are illustrated in Table 8, where results are separated by orientations. The findings showed that, for all directions, the application of coating materials to the wall decreased the decrement factor by 15%–19%. However, it was observed that using coated materials increased the time lag

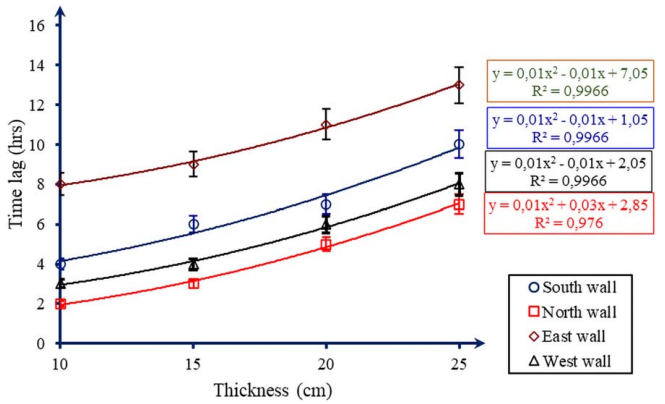

Fig. 8. Influence of wall thickness on thermal time lag for walls with different orientations.

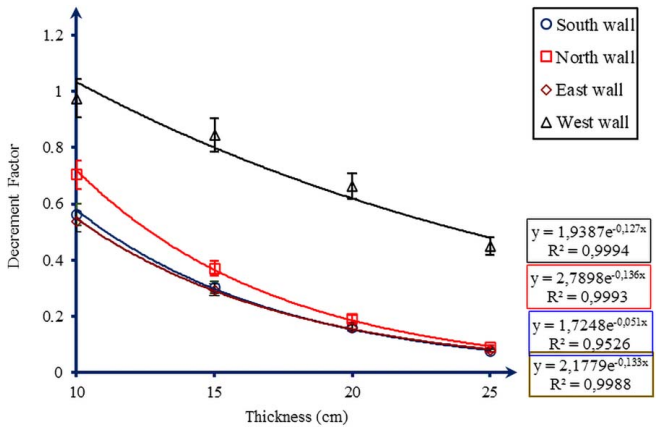

Fig. 9. Influence of wall thickness on thermal decrement factor for walls with different orientations.

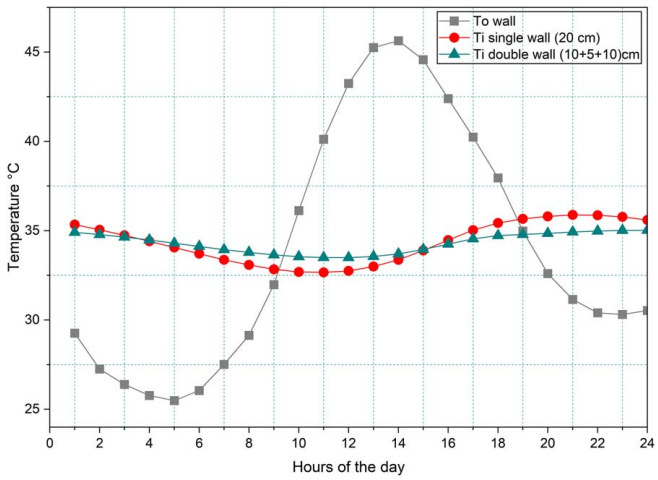

Fig. 10. Effect of air-gap inclusion on daily temperature variations for south-facing walls.

Table 6. Effect of air-gap inclusion on time lag (φ) and decrement factor (f)

Parameter	Single wall = 20 cm	Double wall = (10 + 5 + 10) cm
Decrement factor	0.161	0.101
Time lag (h)	7	9
T_{max} (°C)		
Outer inside	45.63	45.63
Inner inside	35.88	35.32
T_{min} (°C)		
Outer inside	25.49	25.49
Inner inside	32.66	32.28

by 1 h for walls oriented to the south and east and no changes were recorded for walls in the other directions. Thus, it should be indicated that coating rubberized wall with conventional materials, such as cement and plaster, not only improves thermal efficiency but also enhances durability, particularly through the use of exterior cement mortar as a protective layer.

Finally, it should be noted that the rubberized gypsum-based walls gave interesting results in terms of thermal insulation. Nevertheless, the double wall was more advantageous, since it presented lower values of decrement factor in all orientations, as seen in Table 8.

Table 7. Thermal and physical properties of cement and plaster used for coating

Parameter	Cement mortar	Plaster mortar
Thermal conductivity (W/m·K)	1.40	0.5
Heat capacity (J/kg·K)	1,200	1,000
Density (kg/m^3)	2,100	1,300

Table 9 shows the maximum and minimum temperatures, as well as the times of occurrence, for double walls in different orientations. Results confirm that south, north, and east orientations are favorable, while the west is less efficient due to the afternoon solar loads. These findings are consistent with other investigations done in the literature (Huang et al. 2018; Mavromatidis et al. 2012).

Compared with other eco-efficient wall materials such as hempcrete and aerated concrete, the proposed gypsum–rubber composite achieves a distinctive balance between insulation and thermal inertia. Hempcrete offers excellent insulation ($\lambda = 0.09$–0.15 W/m·K) but limited strength (<2 MPa) and time lag ($\varphi = 4$–6 h), while aerated concrete provides moderate strength (3–7 MPa) and conductivity ($\lambda = 0.15$–0.25 W/m·K) but involves energy-intensive production. In contrast, the gypsum–rubber system attains $\lambda = 0.296$ W/m·K and a 9 h time lag for 25 cm walls. An RW content of 20%–30% and wall thickness of 20–25 cm, optionally with a 5 cm air cavity, provide the best compromise between mechanical performance (4–5 MPa) and thermal efficiency for non-load-bearing wall systems.

From a structural engineering standpoint, it is important to highlight that, according to the recommendations of plaster-based construction of CNERIB (1993), the use of plaster-based masonry is permissible in construction, provided that it complies with established technical specifications. The compressive strength of plaster blocks must attain a minimum of 40 kg/cm^2, tested under dry conditions after 28 days of curing, to ensure adequate mechanical performance. Although the use of plaster is not restricted in moderate to high seismic risk zones, the implementation of robust horizontal and vertical reinforcement (anchorage or tie beams) is strongly recommended, consistent with the requirements for other masonry materials in seismic design. Additionally, due to the material's susceptibility to moisture, plaster is best suited for dry climates, particularly in areas characterized by low ambient humidity and minimal rainfall (arid zones). These recommendations primarily concern load-bearing wall systems, but they also extend to other

Table 8. Time lag (φ) and decrement factor (f)

	South		North		East		West	
Type	φ (h)	f	φ (h)	f	φ (h)	f	φ (h)	f
Without coating	9	0.101	9	0.123	12	0.104	7	0.082
With coating	10	0.085	9	0.104	13	0.084	7	0.069
Improvement	+1 h	−15.7%	—	−15.6%	+1 h	−18.9%	—	−15.6%

Table 9. Maximal and minimal temperatures and their hours into the facets of wall

Type of temperature measurement	Wall orientation															
	South				North				East				West			
	T_{max} (°C)	Time	T_{min} (°C)	Time	T_{max} (°C)	Time	T_{min} (°C)	Time	T_{max} (°C)	Time	T_{min} (°C)	Time	T_{max} (°C)	Time	T_{min} (°C)	Time
External	46.31	1400	25.99	0500	40.03	1700	25.94	0500	47.05	1000	26.24	0500	56.12	1700	26.61	0500
Internal	35.58	2400	33.85	1100	35.22	2400	33.76	1200	35.78	2300	34.03	1000	36.14	2400	34.1	1200

structural and nonstructural components such as vaults, plaster blocks, and plaster-based partition elements.

Limitations and Future Works

This study focused on the main aspects of thermal and mechanical performance of rubberized gypsum composites using both experimental and simulation approaches. Other aspects not covered here, such as long-term durability, embodied carbon quantification, and large-scale field validation, could serve as useful directions for future research to provide a broader understanding and stronger practical validation.

Conclusion

The incorporation of RW into gypsum composites successfully produced a lightweight mortar compliant with ACI 213R-87 (ACI 1987) specifications for low-density materials. While mechanical strength decreased with higher rubber content, the composite remains viable for nonstructural applications such as partition walls and prefabricated gypsum panels, aligning with Algeria's Thermal Regulation for Residential Buildings (DTR C3.2, CNERIB 1997). Notably, the addition of 50% rubber waste reduced thermal conductivity by 52% (from 0.615 to 0.296 W/m·K) and thermal diffusivity by 88.6% (from 1.544 to 0.176 mm^2/s), significantly enhancing insulation capacity and enabling energy-efficient construction in arid climates.

Numerical simulations of various wall configurations, based on the climatic conditions of M'sila, Algeria, revealed that increasing the wall thickness to 25 cm significantly improves thermal inertia. In the case of west-facing walls, this configuration reduces the internal surface temperature to 35.6°C, while the external surface temperature reaches 55.5°C, resulting in a temperature attenuation of approximately 36%. This improvement highlights the wall's enhanced capacity to dampen thermal fluctuations, contributing to better indoor thermal comfort and energy efficiency.

East-facing walls exhibited the most stable thermal performance, attributed to lower afternoon solar exposure. The integration of a 5 cm air cavity further improved insulation, decreasing the decrement factor by 38% and increasing time lag by 2 h. Surface coatings (1 cm gypsum interior, 1 cm cement exterior) provided additional gains, mitigating heat ingress through improved emissivity and moisture resistance.

Based on these results, an optimal RW content between 20% and 30% is recommended, as it provides a balanced compromise between mechanical integrity (4–5 MPa) and thermal efficiency. Combined with a 20–25 cm wall thickness and a 5 cm air cavity, this configuration offers the most effective and sustainable design for non-load-bearing wall systems in arid regions.

These findings validate rubberized gypsum composites as a sustainable solution for arid regions, combining waste valorization, local material utilization (e.g., dune sand), and thermal performance optimization. By aligning with circular economy principles and regional building codes, this approach addresses energy poverty and environmental challenges while advancing climate-responsive construction practices.

Data Availability Statement

Some or all data, models, or code that support the findings of this study are available from the corresponding author upon reasonable request.

Acknowledgments

The authors acknowledge the General Directorate of Scientific Research and Technological Development of Algeria (DGRSDT) for its support.

Author Contributions

Hamza Laoubi: Resources, Visualization, Writing—original draft; Abdelaziz Meddah: Conceptualization, Methodology, Supervision, Writing—review and editing; Madani Bederina: Methodology, Writing—review and editing; Abd Elmalik Goufi: Resources.

References

ACI (American Concrete Institute). 1987. *Guide for structural lightweight aggregate concrete*. ACI 213R-87. Farmington Hills, MI: American Concrete Institute.

AFNOR. 1987. *Plasters for normal and extra hard internal finishes, hand or machine applied-classification, designation, specifications.* NF B12-301. Paris, France: AFNOR.

Al-Jabri, K. S., A. W. Hago, A. S. Al-Nuaimi, and A. H. Al-Saidy. 2005. "Concrete blocks for thermal insulation in hot climate." *Cem. Concr. Res.* 35 (8): 1472–1479. https://doi.org/10.1016/j.cemconres.2004.08.018.

Asan, H. 2006. "Numerical computation of time lags and decrement factors for different building materials." *Build. Environ.* 41 (5): 615–620. https://doi.org/10.1016/j.buildenv.2005.02.020.

Badens, E. 1998. "Etude de l'adsorption de l'eau sur les cristaux de gypse et de son influence sur les propriétés mécaniques du plâtre pris pur et additive." *Univ. de Aix-Marseille 3*. Accessed June 14, 2019. http://www.theses.fr.

Belhadj, B., M. Bederina, R. M. Dheilly, L. B. Mboumba-Mamboundou, and M. Quéneudec. 2020. "Evaluation of the thermal performance parameters of an outside wall made from lignocellulosic sand concrete and barley straws in hot and dry climatic zones." *Energy Build.* 225: 110348. https://doi.org/10.1016/j.enbuild.2020.110348.

Belhadj, B., M. Bederina, Z. Makhloufi, A. Goullieux, and M. Quéneudec. 2015. "Study of the thermal performances of an exterior wall of barley straw sand concrete in an arid environment." *Energy Build.* 87: 166–175. https://doi.org/10.1016/j.enbuild.2014.11.034.

Ben Mansour, M., C. A. Soukaina, B. Benhamou, and S. Ben Jabrallah. 2013. "Thermal characterization of a Tunisian gypsum plaster as construction material." *Energy Procedia* 42: 680–688. https://doi.org/10.1016/j.egypro.2013.11.070.

Berardi, U., L. Tronchin, M. Manfren, and B. Nastasi. 2018. "On the effects of variation of thermal conductivity in buildings in the Italian construction sector." *Energies* 11 (4): 1–17. https://doi.org/10.3390/en11040872.

CEN (European Committee for Standardization). 2014. *Binders and plaster-based coatings for building—Part 2: Test methods*. NF-EN 13279-2. Brussels, Belgium: CEN.

CNERIB (National Centre for Studies and Integrated Researches to Building). 1993. *Recommendations for construction with plaster*. [In French.] CNERIB Rep. Ministère de l'Habitat, de l'urbanisme et de la ville. Algiers, Algeria: CNERIB.

CNERIB (National Center for Integrated Building Studies and Research). 1997. *Regulatory technical document in Algeria: Thermal regulation of residential buildings in Algeria—calculation rules for heat losses.* DTR C3-2. Algiers, Algeria: CNERIB.

Debouci, Z., Teggour, H., and Chili, T. 1989. Role of lime in exterior plaster protection. Tipaza, Algeria: Seminar on Plaster Construction, CNERIB.

Deghfel, M., A. Meddah, M. Beddar, and M. A. Chikouche. 2019. "Experimental study on the effect of hot climate on the performance

of roller-compacted concrete pavement." *Innovative Infrastruct. Solutions* 4 (1): 54. https://doi.org/10.1007/s41062-019-0246-8.
Djoudi, A. 2015. "Etude de la durabilité et du comportement thermophonique des bétons de platre renforcés par des fibres végétales du palmier dattier." *ENP d'Alger*. Algiers, Algeria: ENP.
Djoudi, A., M. M. Khenfer, A. Bali, and T. Bouziani. 2014. "Effect of the addition of date palm fibers on thermal properties of plaster concrete: Experimental study and modeling." *J. Adhes. Sci. Technol.* 28 (20): 2100–2111. https://doi.org/10.1080/01694243.2014.948363.
Egenhofer, C., J. C. Jansen, S. J. A. Bakker, and J. J. Hammes. 2006. *Revisiting EU policy options for tackling climate change: A social cost-benefit analysis of GHG emissions reduction strategies*. Brussels, Belgium: Centre for European Policy Studies.
Eldin, N. N., and A. B. Senouci. 1993. "Rubber-tire particles as concrete aggregate." *J. Mater. Civ. Eng.* 5 (4): 478–496. https://doi.org/10.1061/(ASCE)0899-1561(1993)5:4(478).
Erell, E., and Y. Etzion. 1992. "A radiative cooling system using water as a heat exchange medium." *Archit. Sci. Rev.* 35 (2): 39–49. https://doi.org/10.1080/00038628.1992.9696712.
Fathipour, R., and A. Hadidi. 2017. "Analytical solution for the study of time lag and decrement factor for building walls in climate of Iran." *Energy* 134: 167–180. https://doi.org/10.1016/j.energy.2017.06.009.
Ferrández, D., M. Álvarez, A. Zaragoza-Benzal, and P. Santos. 2024. "Eco-design and characterization of sustainable lightweight gypsum composites for panel manufacturing including end-of-life tyre wastes." *Materials* 17 (3): 635. https://doi.org/10.3390/ma17030635.
Guillén, I., V. Gómez-Lozano, J. M. Fran, and P. A. López-Jiménez. 2014. "Thermal behavior analysis of different multilayer façade: Numerical model versus experimental prototype." *Energy Build.* 79: 184–190. https://doi.org/10.1016/j.enbuild.2014.05.006.
Herrero, S., P. Mayor, and F. Hernández-olivares. 2013. "Influence of proportion and particle size gradation of rubber from end-of-life tires on mechanical, thermal and acoustic properties of plaster–rubber mortars." *Mater. Des.* 47: 633–642. https://doi.org/10.1016/j.matdes.2012.12.063.
Ho Anh Cuong, M. 2010. *Optimisation de la composition et caractérisation d'un béton incorporant des granulats issus du broyage de pneus usagés: Application aux éléments de grande surface*. Toulouse, France: L'Insa de Toulouse.
Huang, J., J. Yu, and H. Yang. 2018. "Effects of key factors on the heat insulation performance of a hollow block ventilated wall." *Appl. Energy* 232: 409–423. https://doi.org/10.1016/j.apenergy.2018.09.215.
ISO. 2015. Plastics-Determination of thermal conductivity and thermal diffusivity-Part 2: Transient plane heat source (hot disc) method. ISO 22007-2. Geneva, Switzerland: International Organization for Standardization (ISO).
Jellen, A. C., and A. M. Memari. 2025. "State-of-the-art review of hempcrete for residential building construction." *Designs* 9 (2): 44. https://doi.org/10.3390/designs9020044.
Jiménez Rivero, A., A. de Guzmán Báez, and J. García Navarro. 2014. "New composite gypsum plaster–ground waste rubber coming from pipe foam insulation." *Constr. Build. Mater.* 55: 146–152. https://doi.org/10.1016/j.conbuildmat.2014.01.027.
Laoubi, H., M. Bederina, A. Djoudi, A. Goullieux, R. M. Dheilly, and M. Queneudec. 2018. "Study of a new plaster composite based on dune sand and expanded polystyrene as aggregates." *Open Civ. Eng. J.* 12: 401–412. https://doi.org/10.2174/1874149501812010401.
Laoubi, H., A. Djoudi, R. M. Dheilly, M. Bederina, A. Goullieux, and M. Quéneudéc. 2019. "Durability of a lightweight construction material made with dune sand and expanded polystyrene." *J. Adhes. Sci. Technol.* 33: 2157–2179. https://doi.org/10.1080/01694243.2019.1637091.
Laoubi, H., A. Djoudi, A. Meddah, and M. Bederina. 2017. "Performance thermomécanique d'un béton platre allégé à base de déchets de caouhoutchouc." In *Proc., 3rd Int. Symp. Materials and Sustainable Development*. Cham, Switzerland: Springer Nature.
Mahlia, T. M. I., and A. A. Iqbal. 2010. "Cost benefits analysis and emission reductions of optimum thickness and air gaps for selected insulation materials for building walls in Maldives." *Energy* 35 (5): 2242–2250. https://doi.org/10.1016/j.energy.2010.02.011.
Mavromatidis, L. E., A. Bykalyuk, M. El Mankibi, P. Michel, and M. Santamouris. 2012. "Numerical estimation of air gaps' influence on the insulating performance of multilayer thermal insulation." *Build. Environ.* 49: 227–237. https://doi.org/10.1016/j.buildenv.2011.09.029.
Meddah, A. 2015. *Characterization of roller compacted concrete containing rubber-tire wastes*. Algiers, Algeria: National Polytechnic School of Algiers.
Meddah, A., M. Beddar, and A. Bali. 2014. "Use of shredded rubber tire aggregates for roller compacted concrete pavement." *J. Cleaner Prod.* 72: 187–192. https://doi.org/10.1016/j.jclepro.2014.02.052.
Meddah, A., H. Bensaci, M. Beddar, and A. Bali. 2017. "Study of the effects of mechanical and chemical treatment of rubber on the performance of rubberized roller-compacted concrete pavement." *Innovative Infrastruct. Solutions* 2: 17. https://doi.org/10.1007/s41062-017-0068-5.
Meddah, A., and K. Merzoug. 2017. "Feasibility of using rubber waste fibers as reinforcements for sandy soils." *Innovative Infrastruct. Solutions* 2 (1): 5. https://doi.org/10.1007/s41062-017-0053-z.
Merniz, M., M. Bederina, A. Meddah, L. Pantelidis, and A. Noui. 2025. "An alternative sustainable desert-sand concrete incorporating industrial waste fillers: Physicomechanical and microstructural insights." *Innovative Infrastruct. Solutions* 10: 396. https://doi.org/10.1007/s41062-025-02206-4.
Ministry of Energy. 2015. "New energies, renewables and energy management." Accessed January 15 2019. https://www.energy.gov.dz/?rubrique=energies-nouvelles-renouvelables-et-maitrise-de-lrenergie#518.
Narayanan, N., and K. Ramamurthy. 2000. "Structure and properties of aerated concrete: A review." *Cem. Concr. Compos.* 22 (1): 321–329. https://doi.org/10.1016/S0958-9465(00)00016-0.
Neya, I., D. Yamegueu, Y. Coulibaly, A. Messan, and A. L. S.-N. Ouedraogo. 2021. "Impact of insulation and wall thickness in compressed earth buildings in hot and dry tropical regions." *J. Build. Eng.* 33 (June 2020): 101612. https://doi.org/10.1016/j.jobe.2020.101612.
Oktay, H., Z. Argunhan, R. Yumrutaş, M. Z. Işik, and N. Budak. 2016. "An investigation of the influence of thermophysical properties of multilayer walls and roofs on the dynamic thermal characteristics." *Mugla J. Sci. Technol.* 2 (1): 48–54. https://doi.org/10.22531/muglajsci.269972.
Quagraine, K. A., E. W. Ramde, Y. Atsu, Y. A. K. Fiagbe, and D. A. Quansah. 2020. "Evaluation of time lag and decrement factor of walls in a hot humid tropical climate." *Therm. Sci. Eng. Prog.* 20: 100758. https://doi.org/10.1016/j.tsep.2020.100758.
Raghavan, D., H. Huynh, and C. Ferraris. 1998. "Workability, mechanical properties, and chemical stability of a recycled tyre rubber-filled cementitious composite." *J. Mater. Sci.* 33: 1745–1752. https://doi.org/10.1023/A:1004372414475.
Salih, M. A., and A. Hussian. 2018. "Enhancing the compressive strength property of gypsum used in walls plastering by adding lime." *J. Univ. Babylon Eng. Sci*. 26 (3): 58-66.
Soussi, N., M. Ammar, A. Mokni, and H. Mhiri. 2024. "Thermophysical properties and energy efficiency of a sustainable construction materials produced from local natural waste." *Energy Rep.* 12 (April): 2283–2296. https://doi.org/10.1016/j.egyr.2024.08.025.
Steyn, K., W. de Villiers, and A. J. Babafemi. 2025. "A comprehensive review of hempcrete as a sustainable building material." *Innovative Infrastruct. Solutions* 10: 97. https://doi.org/10.1007/s41062-025-01906-1.
UNEP (United Nations Environment Programme). 2025. "Global status report for buildings and construction 2024–2025: Not just another brick in the wall–the solutions exist." In *Scaling them will build on progress and cut emissions fast*, edited by I. Hamilton and S.-C. Hsu, 13-15. Paris, France: UNEP.
Walker, R., S. Pavia, and R. Mitchell. 2014. "Mechanical properties and durability of hemp-lime concretes." *Const. Build. Mater.* 61: 340-348. https://doi.org/doi.org/10.1016/j.conbuildmat.2014.02.065.
Zhang, Y., K. Lin, Q. Zhang, and H. Di. 2006. "Ideal thermophysical properties for free-cooling (or heating) buildings with constant thermal physical property material." *Energy Build.* 38 (10): 1164–1170. https://doi.org/10.1016/j.enbuild.2006.01.008.